BBA - Molecular Basis of Disease 1870 (2024) 167180

Contents lists available at ScienceDirect

BBA - Molecular Basis of Disease

journal homepage: www.elsevier.com/locate/bbadis

Calcium signaling induces partial EMT and renal fibrosis in a *Wnt4*^{mCherry} knock-in mouse model

Florence Naillat [a,*], Ganga Deshar [a], Anni Hankkila [a], Aleksandra Rak-Raszewska [a], Abhishek Sharma [a], Renata Prunskaite-Hyyrylainen [a], Antti Railo [a], Jingdong Shan [a], Seppo J. Vainio [a,b]

[a] Faculty of Biochemistry and Molecular Medicine, University of Oulu, Finland
[b] Infotech Oulu, Kvantum Institute, University of Oulu, Finland

ARTICLE INFO

Keywords:
Chronic kidney diseases (CKD)
Wnt4
Calcium
Fibrosis
Inflammation
EMT
Kidney
T-cell infiltration

ABSTRACT

The renal tubular epithelial cells (TEC) have a strong capacity for repair after acute injury, but when this mechanism becomes uncontrollable, it leads to chronic kidney diseases (CKD). Indeed, in progress toward CKDs, the TECs may dedifferentiate, undergo epithelial-to-mesenchyme transition (EMT), and promote inflammation and fibrosis. Given the critical role of Wnt4 signaling in kidney ontogenesis, we addressed whether changes in this signaling are connected to renal inflammation and fibrosis by taking advantage of a knock-in *Wnt4*$^{mCh/mCh}$ mouse. While the *Wnt4*$^{mCh/mCh}$ embryos appeared normal, the corresponding mice, within one month, developed CKD-related phenotypes, such as pro-inflammatory responses including T-cell/macrophage influx, expression of fibrotic markers, and epithelial cell damage with a partial EMT. The Wnt signal transduction component β-catenin remained unchanged, while calcium signaling is induced in the injured TECs involving Nfat and Tfeb transcription factors. We propose that the Wnt4 signaling pathway is involved in repairing the renal injury, and when the signal is overdriven, CKD is established.

1. Introduction

Chronic kidney disease (CKD) affects nearly 15 % of Americans and is connected to high morbidity and mortality [1]. CKD leads to irreversible changes in the kidney structures and progressively to the loss of the kidney function. It is induced by acute kidney injury (AKI), such as seen in sepsis, drug exposure, and ischemia [2], and it involves mechanical injuries in renal cells. Wingless-related integration site (Wnt) signaling pathway *via* induction of β-catenin known as the canonical pathway, is a key player in the development of CKD as the signaling is involved in the repair and regeneration of the renal tissue after injury [3]. The tissue response depends on the degree of Wnt–β-catenin activation [3]. If the pathway is activated transiently, it will repair whereas a sustained Wnt- β catenin promotes changes in the renal structure through renal fibrosis, chronic inflammation, and reduction in the capacity to regenerate the injured kidney structures [3,4] .

In renal fibrosis, Wnt-β-catenin is also known to have a role in triggering and sustaining the mechanism of epithelial mesenchymal transition (EMT) which is characterized by the differentiation of the epithelial cells into myofibroblast cells capable of secreting extracellular matrix. This phenomenon is mostly observed in renal tubular epithelial cells (TEC) because these cells are more sensitive to injuries and secrete different Wnt proteins [3–5]. The damaged TEC loses epithelial markers and acquires mesenchymal features. When damaged TECs express both epithelial and mesenchymal markers this is called partial EMT. These cells remain in the tubules with a G2/M phase cell cycle arrest and cannot either regenerate or repair the injured TECs leading to impairment of their functionality. Such is carried out through a wrong set of secreted molecules which further activate the differentiation of interstitial fibroblasts into myofibroblast precursors and induces polarization

Abbreviations: Aqp1, aquaporin 1; BSA, bovine serum albumin; CaM, calmodulin; Ca^{2+}, Calcium; CaN, calcineurin; BUN, blood urea nitrogen; CKD, chronic kidney disease; EMT, epithelial mesenchymal transition; H&E, Hematoxylin & Eosin; LTL, *Lotus Tetragonolobus* Lectin; M&T, Masson Trichome; MT, mutant; PT, proximal tubule; Nfat, Nuclear factor of activated T-cells; TEC, renal tubular epithelial cells; Tfeb, Transcription factor EB; Wnt, Wingless-related integration site; WT, wild type.

* Corresponding author.
E-mail address: Florence.naillat@oulu.fi (F. Naillat).

https://doi.org/10.1016/j.bbadis.2024.167180
Received 13 June 2023; Received in revised form 4 April 2024; Accepted 14 April 2024
Available online 21 April 2024

M2 phenotype and pro-inflammatory activation of macrophages. In return these cells start secreting Wnt ligands that directly reinforce the TECs wrong pattern [4,6]. Partial EMT is the first step of fibrogenic progression leading to CKD and the inhibition of EMT process by blocking Wnt- β-catenin is one of the therapeutic strategies for decreasing renal fibrosis development.

Of the Wnt family, the Wingless WNT4 can be considered one candidate factor for CKD. [7]. *Wnt4* is critical for nephrogenesis [8,9] and is not expressed in the mature functional kidney except in the papilla [10]. However, upon injury, WNT4 expression is induced in the tubular cells and may play a role in tissue repair [10,11] or even in the induction of the fibrosis process [11]. In a CKD cohort, some evidence shows that the expression of the *WNT4* gene depends on the stage of CKD, with higher expression in the later stages [12]. Such results raise the hypothesis that *Wnt4* could play a role in the TECs to rescue the establishment of CKD. We used the engineered knock-in *Wnt4*$^{mCh/mCh}$ transgenic mouse to address this. We provide evidence that the deregulated Wnt4 signaling in these mice altered kidney functions toward fibrosis *via* noncanonical Wnt pathway. This mouse model helps us to understand the stemming of the CKD development.

2. Methods

2.1. Mouse lines and urine collection

Wnt4$^{mCh/mCh}$ mouse line was generated and maintained [13] according to the guidelines of the University of Oulu. The Animal Welfare and Ethical Review Body approved all mouse experimental procedures at Oulu University following the Animals Act 1986 (Scientific Procedures). The animal experiments were also approved by the Finnish National Animal Experiment Board (permit numbers ESAVI/18215/2019 and ESAVI/32696/2023) and conducted at the Laboratory Animal Centre of the University of Oulu (OULAC). The sexes of the embryos and pups were not determined, and thus the samples contained both females and males in randomized ratios for all the analyzed stages in this study.

The urine collection was carried out under the authorized mouse license (ESAVI/21036/2019). In brief, the mice were placed individually in metabolic cages for 12 h, where food was removed. Water was available to the mice. Blood was collected when the mice were euthanized. Urine and blood biochemical tests were analyzed at the Medical Research Council Harwell, Mary Lyon Centre, UK. The Blood urea nitrogen and creatine clearance were calculated according to Rodriguez et al. 2014 [14].

2.2. MDCK cell lines and primary renal TECs-cultures

Wnt4Flag, Wnt4mCherryFlag, mCherry, and *nephrinFlag* plasmids [15,16] were transfected by electroporation using Neon® Transfection System (Thermo Fisher Scientific, USA), with a pulse of 1650 for 20 ms in MDCK cell line gift from Dr. Aki Manninen, (University of Oulu). MDCK cells were grown in MEM medium (Gibco Life Technology, UK) supplemented with 10 % FBS (Sigma, USA) and 1 % penicillin/streptomycin (Sigma, USA). NIH 3 T3 cell line overexpressing *Wnt4* gene [9] were grown in DMEM1X + GlutaMax+ D-Glucose+ Pyruvate (Gibco Life Technology, UK) supplemented with 5 % FBS and 1 % Penicillin and Streptomycin (Sigma, USA) in incubator at 37 °C, 5 % CO_2. *Wnt4* NIH3T3 cells were cultured as described before [8,16].

Primary TECs cultures from mouse WT and *Wnt4*$^{mCh/mCh}$ mouse kidneys were carried as described by Ding et al. [17] except that the mice were not perfused. The kidney capsule, renal medulla, and pelvis were removed as soon as the kidneys were harvested. The rest of the kidneys were minced and incubated in trypsin-collagenase type-2 (Sigma, USA) in PBS [18] and rotated for 15–30 min at 37 °C. The digested solution was passed through a 70-μm filter (Corning, Life Sciences, USA), and 5 ml of medium DMEM:F-12 (Gibco Life Technology, UK) was added to stop the enzyme reaction. The solution was centrifuged at 500*g* for 5 min, and the pellet was collected. The pellet was resuspended in 2 ml of medium (Gibco Life Technology, UK). TECs at a concentration of 10^7 live cells (live cell population was checked using TC20™ Automated Cell Counter, Bio-Rad) were cultured onto collagen-coated plate in DMEM:F-12 (Gibco Life Technology, UK) supplemented with 5 % FBS (Sigma, USA), 1 % penicillin-streptomycin (Sigma, USA), 10 ng/ml of epidermal growth factor (H-EGF 236-EG-200, R&D, USA), 5 μg/ml of insulin (I0516, Sigma, USA), 1 % ITS and 1 % Non-essential Amino acids (Sigma, USA) and incubated 37 °C, 5 % CO2. The cultures were treated with cyclosporin (10 μM, gifted from Prof Risto Kerkela, University of Oulu), and XAV939 (2 μM, gifted from Prof Lari Lehtiö, University of Oulu) for 48 h in incubator at 37 °C, 5 % CO_2.

For the induction assay by *Wnt4*$^{mCh/mCh}$ TECs, the *Wnt4*$^{mCh/mCh}$ dissociated kidney cells were seeded (at 40×10^6 cells) at the bottom of a cell culture plate. Hanging cell culture insert, where WT dissociated TECs were seeded with a concentration of 10×10^6 cells, was suspended on top of the cell culture plate. The co-culture assay was incubated in DMEM:F-12 (Gibco Life Technology, UK) supplemented with 5 % FBS (Sigma, USA), 1 % penicillin-streptomycin (Sigma, USA), 10 ng/ml of epidermal growth factor (H-EGF 236-EG-200, R&D, USA), 5 μg/ml of insulin (I0516, Sigma, USA), 1 % ITS and 1 % Non-essential Amino acids (Sigma, USA) for 48 h in an incubator at 37 °C, 5 % CO_2.

2.3. Cell culture

pcDNA3 *Wnt4IresGFP* construct was transfected to the mk3 cells [19] with TurboFect transfection reagent (ThermoFisher Scientific, Lithuania). GFP positive cells were sorted three times to generate stable cell line using BD FACSARIA™ (BD Bioscience). The mk3 and the *Wnt4* mk3 cells were cultivated in low glucose DMEM (Gibco Life Technology, UK) with 10 % FBS (Sigma, USA) and 1XPenicil/streptomycin (Sigma, USA). When reaching 90 % confluence, cells were washed with Hank's Balanced Salt Solution (HBSS, Sigma-Aldrich, Canada) at 37 °C, incubated in starving medium low glucose DMEM, 0 mM Ca^{2+} with 0.1 % BSA for 30 min and finally treated with 4 mM [Ca^{2+}] (Sigma-Aldrich, USA) or 2 mM EGTA (Sigma-Aldrich, USA) for 2 h. After treatment, cells were washed three times with ice cold phosphate-buffered saline (PBS) without Ca^{2+}. 400–500 μl of lysis buffer supplied with proteinase inhibitor cocktail (Roche, Basel, Switzerland) was used to lyse cells for 30 min in ice with frequent vortex, followed by centrifugation to pellet cell debris. Cleared cell lysates were measured for protein concentration and Bradford calculated for loading protein on WB gel for 50 μg of protein.

2.4. Three-dimensional culture of MDCK cells, staining

MDCK and *Wnt4flag*, *Wnt4mCherryflag,* and *mCherry* overexpressing MDCK cells were cultured in Matrigel (354,277, Corning Life Science); approximately 20,000 cells/ml were used to form bulbs in 24 well plates. The cells with matrigel mix were allowed to be set in an incubator for 1 h at 37 °C. After 1 h, 500 μl of warm media MEM (Gibco Life Technology, UK), 5 % FBS (Sigma Life Science, USA), 1 % Penicillin, and Streptomycin (Sigma Life Science; USA) were added to each well and incubated at 37 °C with 5 % CO_2. Every two days, the media was removed and changed with new media without disturbing the bulbs. The culture was set to grow for a week at least. After one week, the culture was fixed with 4 % paraformaldehyde (Sigma Aldrich, USA) and stained with antibodies Wnt4 (MAB4751, R&D System), mCherrry (AB167453, Abcam), Anti-Flag (F3165, Sigma), Phalloidin TRITC/Phalloidin 488 (A12380, A12379, Sigma, USA) and the secondary antibodies (Alexa Fluor, Thermofisher Scientific) [20] were used according to the host of the primary antibody. Confocal images were acquired using a Zeiss LSM 780 laser scanning confocal microscope (Zeiss, Germany). Consecutive stacks were imaged. For counting cysts with lumen, no lumen, or multilumen, *Z*-stack was chosen with optimization of sectioning with intervals of 1–3, the smallest section of 0.5 μm increments [15].

2.5. TOPFlash assays

A Wnt reporter assay was performed according to Railo et al. [20]. For this, pcDNA3-Wnt4, pcDNA3-Wnt4-mCherry, SuperTopFlash, or CMV-β-Gal plasmids were used [20]. The amount of DNA per well was adjusted to 350 ng with the pcDNA3 DNA and transfected to Chinese hamster ovary (CHO) cells. The CHO cells were harvested 24 h later into a cell culture lysis reagent (Promega, USA). A luciferase assay system kit (Promega, USA) and β-galactosidase staining were the indicators and quantified with a Victor3V multilabel counter (PerkinElmer, USA).

2.6. Real-time RT-PCR

RNA was extracted from cell lines and kidneys from *Wnt4*$^{mCh/mCh}$ and WT mouse using Trizol reagent [18] and 0,5-1 μg RNA was reverse transcribed for synthesis of cDNA following cDNA synthesis Kit (ThermoScientific, UK). Real-time qPCR was performed using Brilliant III SYBR Green Master Mix (Agilent Technologies) and the BioRad CFX96 Real-time system with C1000 Touch Thermal Cycler. Glyceraldehyde-3-phosphate dehydrogenase (Gapdh) was used for normalization and primer pairs for *Wnt4*, *mCherry*, *Gsk3*, β-*catenin*, *Wnt5*, *Wnt9b*, *Wnt11*, *Axin2*, *Dkk1* were from publications [13,21]. The data was analyzed by Bio-Rad CFX manager. The sequences of primer used are listed in Supplementary Table 1.

2.7. Tissue preparation, histology and staining

Wnt4$^{mCh/mCh}$ and WT kidney samples were isolated from mice. Samples were fixed in 4 % PFA overnight at 4 °C and washed with sterile PBS$^{-/-}$ overnight (O/N). Then, ethanol grading was performed by adding ethanol concentrations from 30 %, 50 %, and 70 % for at least O/N per sample at 4 °C. The ethanol re-grading was achieved from 80 % to 0 % in Tissue processor Vip5 Junior (Sakura, Japan) O/N. The samples were then embedded in paraffin (Tissue embedding console Tissue-Tek, Sakura Finetek) and stored at 4 °C. The samples were sectioned 6 μm thick for the newborn stage and 3 μm for one- and 3-month-old kidney on a cryostat, and the sections were stored at 4 °C. Sections were stained with Hematoxylin and Eosin (H&E) staining and Masson Trichome (M&T) staining [22].

2.8. In situ hybridization

The non-radioactive *in situ* hybridization analysis of *Wnt4, Slc34a1, Nkcc, Six2,* and *Wnt9b* expression was carried out, as described earlier [22]. A minimum of three kidney-derived sections for each genotype and stage were examined for the respective genes.

2.9. Optical projection tomography

Specimens for optical projection tomography (OPT) were prepared as described earlier in Prunskaite-Hyyryläinen [23]. Shortly, collected E18.5 kidneys of *Wnt4*$^{mCh/mCh}$ and WT mice were processed for whole immunostaining as defined earlier by Nagy et al. [24]. Troma antibody (Developmental Studies Hybridoma Bank) was used as the primary antibody, followed by 488 Alexa fluor secondary antibody. Whole-mount immuno-stained kidneys were embedded in 1 % low melting point agar, dehydrated in a stepwise manner with serial dilutions of EtOH mixed with PBS for 12 h, and cleared in benzyl alcohol/benzyl benzoate (1:2) solution for at least 24 h. Imaging was performed on the OPT Scanner 3001 M (Bioptonics Microscopy, UK) in Biocenter Oulu Tissue Imaging Center at Oulu University, Finland. Images were reconstructed using NRecon (Skyscan Pty Ltd., Kontich, Belgium) software 1.7.1.0. The Imaris software v9.2.1 (Bitplane, Zurich Switzer- land) was used to analyze the OPT data.

2.10. Measurement of oxygen consumption rate

A Seahorse Bioscience Seahorse XFp extracellular flux analyzer (Agilent, USA) was used to measure the rate change of dissolved O_2 in a medium immediately surrounding TECs cells. Mouse primary TECs were seeded in XFp cell culture miniplate (Seahorse Bioscience) at 40×10^4 cells per well and cultured for 24 h, as mentioned above. Oxygen consumption rate (pmol min^{-1}) was assessed using the Seahorse XFp Cell Mito Stress Test Kit (Agilent, Seahorse Bioscience). The generated data was analyzed using the Seahorse XFp Analyzer software (Agilent, USA).

2.11. Western blot analysis

Wnt4$^{mCh/mCh}$ and WT kidneys were dissected, snap-frozen in liquid nitrogen, and stored at −70 °C. Western blot assays followed Veikkolainen et al. protocol [22]. Proteins from cell lines and tissue samples were homogenized in RIPA lysis buffer with phosphatase inhibitor (Sigma, USA), and protein assay was performed using BCA Protein Assay Kit Pierce ™ (Thermo-scientific, USA). 50 μg of protein samples were loaded on 12.5 % SDS gel. The primary antibodies (Supplementary Table 2) were added in the blots and incubated overnight at 4 °C. Then, respective horseradish peroxidase-conjugated secondary antibodies were added at room temperature. The bands were visualized using a chemiluminescent substrate (Lumiglow reagent, Cell Signaling Technology), and imaging was done in Fujifilm LAS-3000 Luminescent Image Analyzer (Raytek Scientific ltd). The bands of the western blot gels were quantified using ImageJ software.

2.12. Flow cytometry

After the sacrifice of *Wnt4*$^{mCh/mCh}$ and WT mice, kidneys were removed, placed into a petri dish, cut into small pieces using a scalpel, and passed through a 70 μm strainer (Corning, Life Sciences, USA). Cells were suspended in 25 ml of media (DMEM media (Gibco Life Technology, UK), 5 % FBS (Sigma, USA), 1 % antibiotic mix (Sigma, USA)). Samples were centrifuged 400 ×*g* at 4 °C for 10 min to pellet the cell suspension. The pellet was resuspended in 4 ml of 40 % Percoll solution (Sigma Aldrich, USA) and gently overlayed onto the 4 ml of 80 % Percoll solution with a transfer plastic pipette very slowly and carefully. This step resulted in two phases separated by a translucent layer. Samples were centrifuged at 1500*g* for 30 min at room temperature with the centrifuge in brake-off mode. The thick yellow top layer of about 1–2 ml was removed by aspiration and the interface of the two phases was collected (~ 2 ml) and mixed with 13 ml of medium (DMEM media (Gibco Life Technology, UK), 5 % FBS (Sigma, USA), 1 % antibiotic mix (Sigma, USA)) to make a total volume of 15 ml. Samples were centrifuged at 400*g* for 10 min at 4 °C and a cell pellet was collected. The cells were then stained with surface markers in PBS (ThermoFisher Scientific, USA) with 1 % FBS (Sigma, USA) and incubated at 4 °C for at least 1 h. Samples were centrifuged at 1500–3000 rpm at 4 °C for 5 min and the supernatant was removed. Cells were washed with PBS-1 % FBS. Fixation and permeabilization solution (BD Bioscience) were added to the cells and incubated for 20 min at 4 °C. Cells were washed two times in 1× BD Perm/wash buffer solution (BD Bioscience). The pellet was resuspended in the BD Perm/wash buffer solution (BD Bioscience) containing intracellular cytokines and incubated at 4 °C for 30 min. Cells were washed twice with 1× BD Perm/wash buffer and resuspended in staining buffer before flow cytometry [25]. The following antibodies were used anti mouse- CD45-PE Cy7 (1800-17, Southern Biotech), CD8-PE (Clone 53-6.7), CD4-APC (Clone RM4-5), CD11b-PE (Clone M1/70) (BD Pharmingen), CD3-FITC (clone 145-2C11), TNFα-Alexa 488 (Clone MP6-XT22), INFY-Alexa 488 (Clone XMG1.2) (BD Bioscience), IL-10-Alexa 488 (FAB53681G), IL-27-fluorescein (Clone # 26350, FAB21091F, R&D System), CD86-Pacific blue (Clone GL-1), CD163-APC (Clone S15049I, BioLegend). Primary antibodies alpha-SMA (A2547, Sigma), Toma-I (DSHB, USA), Wnt4 (MAB4751, R&D System), and pH 3

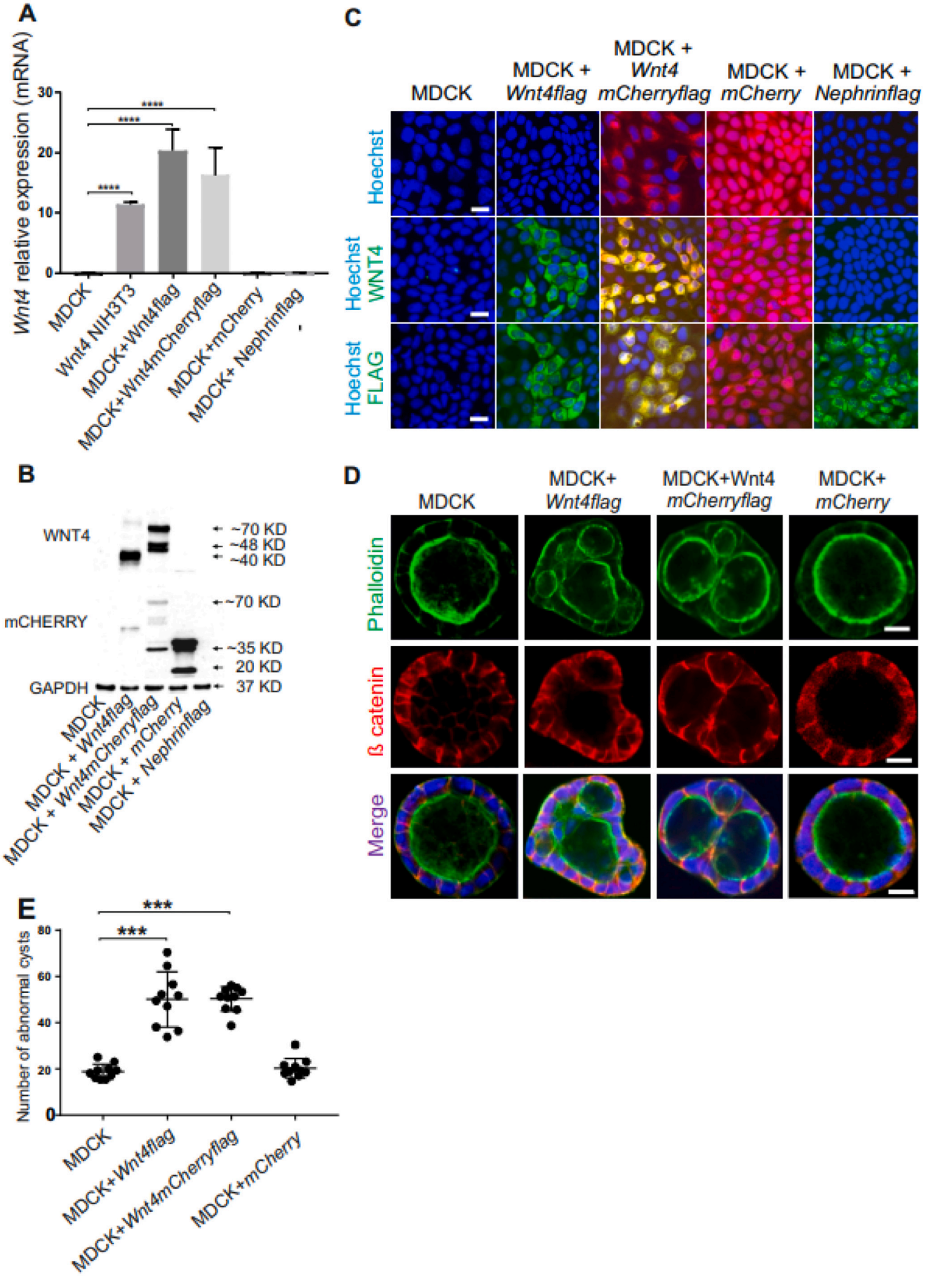

(caption on next page)

Fig. 1. Overexpression of WNT4 disrupts epithelial cell polarization in *in vitro,* causing cystogenesis. A) Relative expression of *Wnt4* mRNA in transfected MDCK cells (*Wnt4flag*, *Wnt4mCherryflag*, *mcherry*, *Nephrinflag*, ($n = 4$)). B) Western blot analysis of WNT4 and mCHERRY protein in MDCK cells. WNT4 protein (~50 kDa) was highly expressed in transfected MDCK cells with *Wnt4flag* and *Wnt4mCherryflag* constructs (~70 kDa full-size fused protein, ~50 kDa Wnt4 protein) (A, B). For mCHERRY protein, two bands can be visualized (~70 kDa full size fused protein, ~50 KDa WNT4 protein) and a third one (~35 kDa) as mCHERRY protein can hydrolyze its main chain at the acylimine linkage [16] C) Staining of β-catenin, Wnt4, flag protein in MDCK cells. D) Staining of cysts after 1-week culture using Hoechst (blue), phalloidin 488 (green) and β-catenin (red). C—D) Scale bar 20 μm. e) Number of cysts with abnormal lumens. Cysts were counted and classified as normal (single central apical lumen) whereas abnormal (no lumen or poorly characterized lumen, multiple lumen) ($n = 10$, minimum 200–300 counted cysts per sample). Data are represented as mean ± s.e.m. A, E) Two-way analysis of variance (ANOVA) with Dunnett's multiple comparison test, p**** < 0.0001.

(06-570, Merck Millipore, USA) were used followed by corresponding fluorescent secondary antibodies. Samples were sorted using BD LSRFortessa™ Cell Analyzer (BD Biosciences, USA). The FlowJo software v 10.8.1 (BD Biosciences) was used for gating and analyzing the data.

2.13. Immunostaining

MDCK cells were cultured on clean circular glass coverslips in a 12-well plate and incubated at 37 °C with 5 % CO_2. The cells were then fixed with 4 % paraformaldehyde (PFA) solution for 20 min at room temperature, washed with $PBS^{-/-}$ (Sigma, USA) for 5 min, 3 times, and 800 μl of blocking solution PBST (10 % FBS (Sigma, USA), 0.1 % Triton (Sigma, USA) in 1× PBS) was added followed by incubation at room

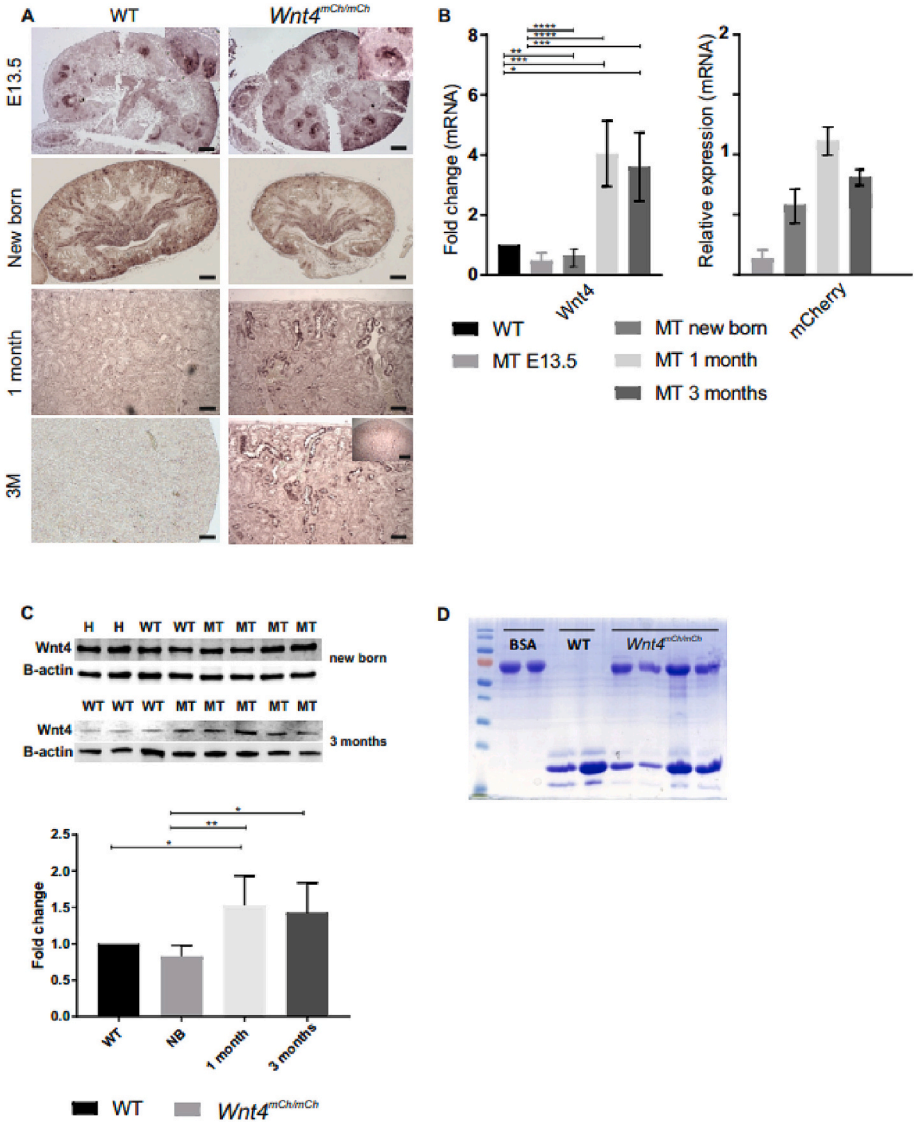

Fig. 2. Wnt4 expression in adult kidneys alters kidney functions. A) *Wnt4 in situ* hybridization of WT and $Wnt4^{mCh/mCh}$ kidneys at E13.5, newborn, 1- and 3-month-old mice. Scale bar, 500 μm. ($n = 6$ for each genotype at E13.5 and newborn stage, $n = 5$ at 1-month-old and $n = 3$ at -months-old). B) *Wnt4* and *mCherry* mRNA expression in kidneys at E13.5, newborn, 1-month-old, and 3-month-old mice. (n = 6 for each genotype, except for 3-month-old n = 3 for the $Wnt4^{mCh/mCh}$ genotype) C) WNT4 protein expression in newborn and 3-month-old kidneys. Western blot (up) and quantitation (down) of one-quarter of the kidney H heterozygote, WT wild-type, MT mutant (Newborn stage $n = 2$ for WT/$Wnt4^{mCh}$, n = 2 for WT and $n = 4$ for $Wnt4^{mCh/mCh}$; 3 months n = 3 for WT and n = 5 for $Wnt4^{mCh/mCh}$). D) Urine analysis of WT and $Wnt4^{mCh/mCh}$ kidneys by western blot assay. BSA (bovine serum albumin) is loaded as a reference (68 KD) (n = 2 for WT and n = 4 for $Wnt4^{mCh/mCh}$). B, C) Data are represented as mean ± s.e.m., Two-way analysis of variance (ANOVA) with Tukey post-hoc analysis test P* <0.05, P** < 0.01.

temperature for 30 min. Then, primary antibodies were added and incubated overnight at 4 °C. The next day, the samples were washed with PBST, and respective fluorescent secondary antibodies were added for 1 h at room temperature and Thermo Scientific™ Shandon™ Immu-Mount™ (Fisher Scientific, USA) was added on top of the slide (Supplementary Table 2). The imaging was done under 20× magnification in an Olympus FluoView FV1000 confocal Microscope (Olympus, USA).

2.14. Calcium measurement

Calcium of TECs cultures was measured by Fluo-4 staining (Thermo Fisher Scientific, USA) according to the supplier's protocol with a STELLARIS 8 FALCON FLIM confocal microscope (Leica Microsystem, Germany Gmbh) in Hank's solution (Gibco Life Technology, UK). Calcium storage was measured with 10 μM injection of ionomycin (Sigma, USA) that disrupts the endoplasmic reticulum (ER), causing calcium to flow into the cytoplasm. Calcium release speed was measured with 2 μM thapsigargin (ThermoFisher Scientific, USA) injection that prevents calcium from being transported back to ER.

2.15. Statistical analysis

For comparisons between two groups, statistical significance was determined using the 2-tailed Student's *t*-test and for all quantitative comparisons, two-way ANOVA with Bonferroni's or Sidak multiple comparisons test was performed with GraphPad Prism 7.03 software. $P \leq 0.05$ and lower values were considered statistically significant, and the results were presented as mean standard error. Asterisks indicate statistical significance according to this legend: $*P < 0.05$: $**P < 0.01$; $***P < 0.001$.

3. Results

3.1. Wnt4 gain of function deregulates polarization and promotes cyst formation in the Mardin Darby Canine Kidney cells

The Mardin Darby Canine Kidney (MDCK) kidney epithelial cells were used as an *in vitro* model for tubulogenesis and cystogenesis [15]. The cells were transfected with the *Wnt4flag, Wnt4mCherry, mCherry,* and Nephrin flag constructs [16], and the *Wnt4* expressing NIH 3T3 cells served as a positive control [8]. The *Wnt4 flag* and *Wnt4mCherry* flag transfected MDCK cells expressed the *Wnt4* mRNA and protein (Fig. 1A, B). Both *mCherry* mRNA and proteins were present in the transfected MDCK cells with the expected protein sizes [16] (Fig. 1B). Moreover, the WNT4, mCHERRY, and FLAG proteins were identified in the cytoplasm of the transfected MDCK cells (Fig. 1C). In 3D culture, the MDCK cells form epithelial cysts and develop a lumen [15]. Around 50 % of the *Wnt4flag* and *Wnt4mCherry flag* transfectants exhibited abnormal cysts, while in the control MDCK and *mCherry* transfectants, the number was around 20 % (Fig. 1D-E). Overexpression of WNT4 in MDCK leads to cystogenesis.

3.2. The kidney is impaired in the $Wnt4^{mCh/mCh}$ adult mice

To study the noted MDCK anomalies *in vivo*, we generated a mouse line where a fusion protein between *Wnt4* and *mCherry* was inserted into the first exon of the *Wnt4* locus and was named the $Wnt4^{mCh}/^{mCh}$ allele [13]. No differences were noted in the embryonic or placental weight (Supplementary Fig. S1A,B), and no striking phenotypes between the wild type (WT) and $Wnt4^{mCh}/^{mCh}$ embryos at E13.5 and E18.5 were observed. The gross morphology of each organ contained the differentiated structures needed for the organ functionality (Supplementary Fig. S2A-D). The qPCR results for the *Wnt4* mRNA expression were upregulated in the liver, lungs, heart, and spleens of the $Wnt4^{mCh}/^{mCh}$ embryos, except for adrenal glands and kidneys, where the expression was reduced (Supplementary Fig. S2B-D). These results suggest that in the adrenal glands and kidneys the necessary level of WNT4 protein is achieved to form all the structures in the organs which might explain why these mice survive after birth until 9 month-old. In the $Wnt4^{mCh}/^{mCh}$ mice-derived adult organs, a similar trend for the *Wnt4* expression was observed as in the embryos (Supplementary Figs. S3, S4). However, the spleen/kidney/body weight ratio remained smaller in the $Wnt4^{mCh}/^{mCh}$ mice than in controls while the rest of the organs had a normal organ/body weight ratio (Supplementary Fig.S3, S5). No sex-related differences were noted except for the reproductive organs (manuscript in preparation).

Table 1
Summary of the renal function of WT and $Wnt4^{mCh/mCh}$ mice of 1–2 mnth-old. ($n = 6$ for each genotype).

Parameters	WT	$Wnt4^{mCh/mCh}$
Blood		
Sodium (mmol/l)	145 +/− 3	148 +/− 7
Chloride (mmol/l)	111 +/− 2.65	109 +/− 6.7
Potassium (mmol/l)	5.6 +/− 1.64	4.3 +/− 0.37
Calcium (mmol/l)	2.35 +/− 0.13	2.16 +/− 0.6
Urea (mmol/l)	9.65 +/− 0.65	34.13 +/− 18.3**
Plasma creatinine (μmol/l)	10.93 +/− 4.42	31.05 +/− 13.99**
Urine		
Sodium (mmol/l)	108 +/− 20.25	86 +/− 47.1
Chloride (mmol/l)	148 +/− 38.64	102 +/− 57.1
Potassium (mmol/l)	187 +/− 65.45	107 +/− 34.83*
Magnesium (mmol/l)	18.9 +/− 4.91	12.29 +/− 2.37*
Urea (mmol/l)	910 +/− 196	579 +/− 231**
Creatinine (μmol/l)	2067.5 +/− 356.6	1534.1 +/− 763.3
BUN (mg/dl)	26.40 +/− 1.79	122.31+/− 50.25*
Creatinine clearance (μl/min)	141.08 +/− 44.14	28.65 +/− 10.93**

T-test non parametric * $p < 0.05$, ** $p < 0.01$.

3.3. $Wnt4^{mCh/mCh}$ knock-in leads to hypoplastic kidney and altered kidney functions

The generated $Wnt4^{mCh/mCh}$ adult mice and their kidneys were notably smaller than the controls (Supplementary Fig. S3). A panel of nephrogenesis genes *Slc34a1*, *Nkcc*, *Six2*, and *Wnt9b* genes at E16.5 stage were typically expressed irrespective of the $Wnt4^{mCh}/^{mCh}$ function, and the number of glomeruli remains unchanged in the kidneys of newborn mice (Supplementary Fig. S6). At one and three months, the kidneys of $Wnt4^{mCh/mCh}$ mice were reduced in size and had altered overall morphology, containing fluid-filled cysts in part, not noted in the controls (Supplementary Fig. S3). We did not identify cysts at E18.5 with the optical projection tomography (Supplementary Fig. S7), indicating that they presumably appeared after birth. In line with the cyst formation in the MDCK cells overexpressing the *Wnt4* gene, the *Wnt4* RNA was highly expressed in the kidney cortex and medulla after the birth due to the $Wnt4^{mCh/mCh}$ expression (Fig. 2A-C).

We progressed to study kidney functions of $Wnt4^{mCh/mCh}$ mice and collected urine in which we depicted notable proteinuria in the $Wnt4^{mCh/mCh}$ samples (Fig. 2D). Renal functions were also affected as the plasma and urine creatinine were significantly altered. The blood urea nitrogen (BUN) was high, and the creatinine clearance was low in the $Wnt4^{mCh/mCh}$ mice compared to WT mice, confirming the kidney damage (Table 1). We hypothesize that mCHERRY could interfere with the folding of the WNT4 protein. To answer such question, we generated a homology model of the $WNT4^{mCherry}$ fusion protein based on the Xenopus WNT8 protein using I-TASSER server [26]. The predicted homology model suggested that the direct tagging of mCHERRY to WNT4 causes structural changes in the receptor binding domain, leading to steric hindrance, and this may be relevant in deregulating Wnt4 signaling and driving the observed kidney anomalies (Supplementary Fig. S8).

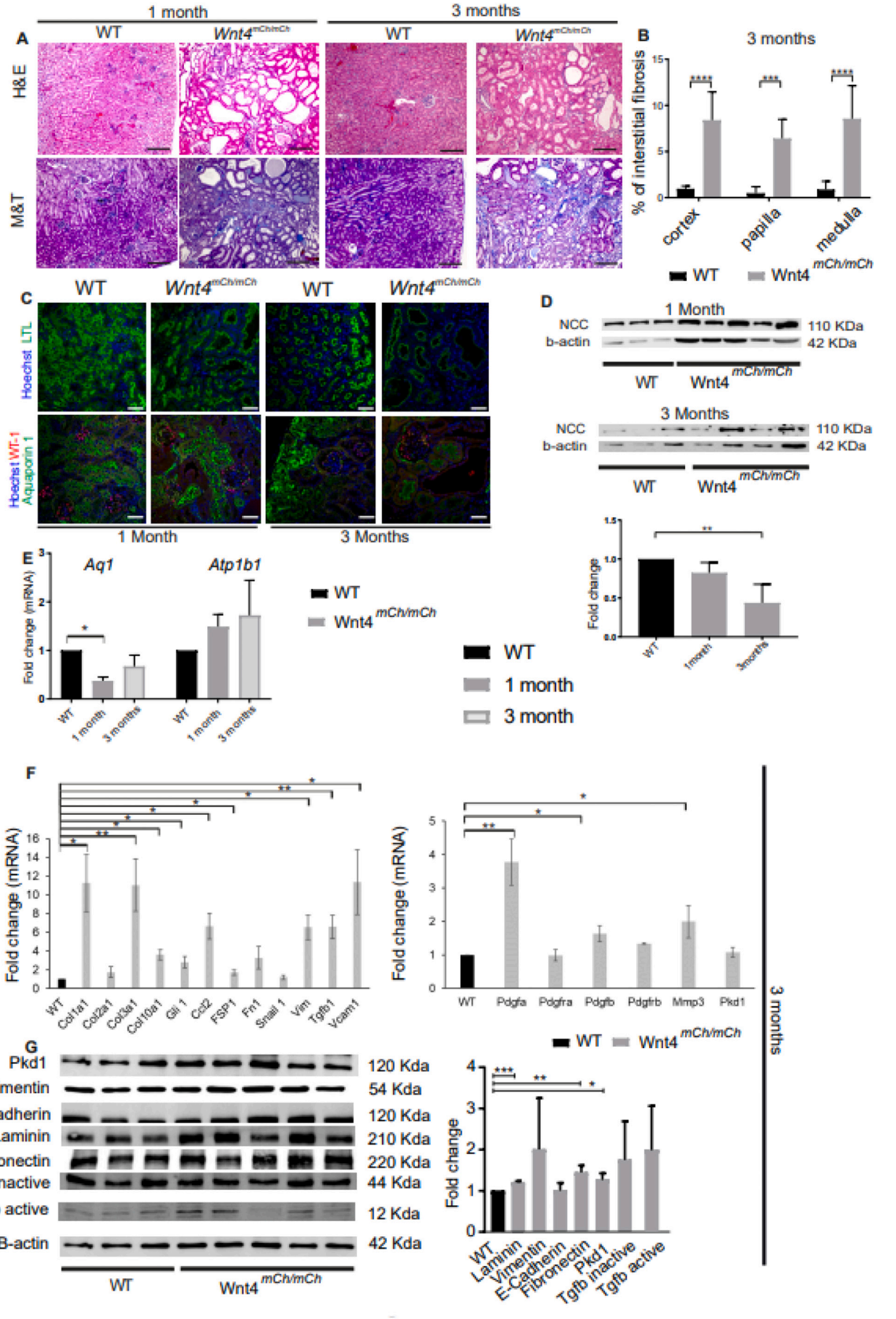

(caption on next page)

Fig. 3. Genetic targeting of Wnt4 signaling induces EMT and fibrosis. A) Representative images of WT and *Wnt4*$^{mCh/mCh}$ kidneys stained with Hematoxylin & Eosin (H&E) and Masson Trichome staining (M&T) at different stages 1- and 3-month-old mouse kidneys ($n = 4$ for each genotype). Scale bars, 100 μm. B) Quantification of the percentage of fibrotic cells based on M&T staining at 3-month-old mice (n = 4 for each genotype). C) Representative images of immunolabeling for LTL and Hoechst, and Wilms tumor 1 (WT1), Aquaporin-1, and Hoechst in WT and *Wnt4*$^{mCh/mCh}$ stained kidneys. Scale bars, 200 μm. (n = 4 for each genotype). D) NCC protein expression in 1- and 3-month-old kidneys. Western blot (up) and quantitation (down) of one-quarter of the kidney. ($n = 3$ for WT and $n = 5$ for *Wnt4*$^{mCh/mCh}$). E, F) Fold change of the indicated genes in *Wnt4*$^{mCh/mCh}$ kidneys compared to WT kidneys (n = 4 for each genotype) G) Protein expression of selected genes in 3-month-old kidneys. Western blot (left) and quantitation (right) of one-quarter of the kidney. (n = 3 for WT and n = 5 for *Wnt4*$^{mCh/mCh}$). For panel D-G, data are presented as mean ± s.e.m.; Two-way ANOVA with Tukey post-hoc analysis is used. *$P < 0.05$, **$P < 0.01$, ***$P < 0.001$. b) Unpaired two-tailed *t*-test. P**** < *0.0001,* P*** < 0.001.

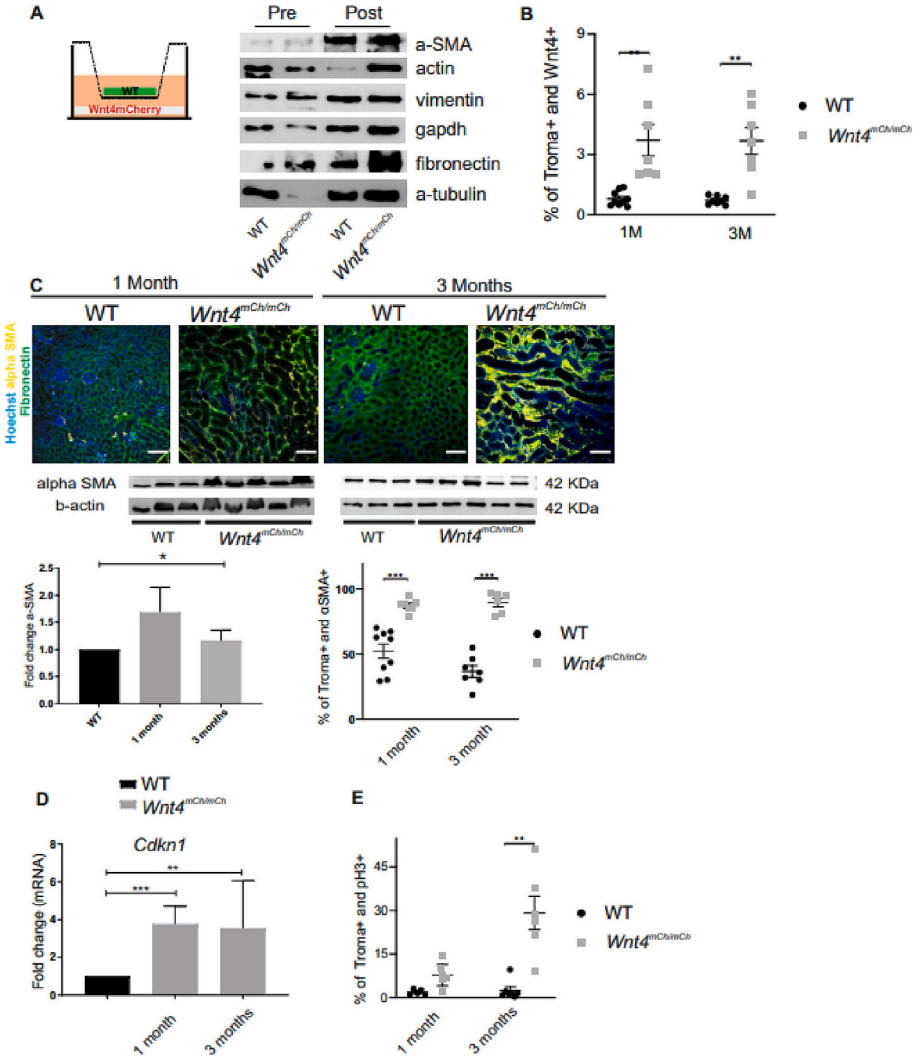

Fig. 4. An EMT program is associated with deregulated expression and functionality of TECs with G2 cell cycle arrested cells. A) Induction of fibrosis genes in WT TECs culture by Wnt4 in the *Wnt4*$^{mCh/mCh}$ TECs visualized by western blot. ($n = 6$ for each genotype). B) Percentage of sorted Troma+Wnt4+ cells in kidneys from WT and *Wnt4*$^{mCh/mCh}$ mice. (n = 6 for each genotype). C) Representative images of immunolabeling for α-SMA, Fibronectin, and Hoechst in 1- and 3- month-old kidneys ($n = 4$ for each genotype). Western blot and quantitation of α-SMA protein in one-quarter kidney ($n = 3$ WT and $n = 5$ for *Wnt4*$^{mCh/mCh}$). Percentage of sorted α-SMA + Troma+ cells in 1- and 3-month-old kidneys (n = 6 for each genotype). Scale bar, 200 μm. D) Fold change of Cdkn1 in WT and *Wnt4*$^{mCh/mCh}$ kidneys (n = 6 for each genotype). E) Percentage of sorted Troma+pH 3+ cells in 1- and 3-month-old kidneys. (n = 6 for each genotype).

3.4. *Fibrogenesis and partial EMT in the kidneys of the Wnt4*$^{mCh/mCh}$ *mice*

We then analyzed the kidney appearance and possible changes in collagen deposition at post-natal stages in more detail. The adult kidneys of *Wnt4*$^{mCh/mCh}$ mice developed fibrotic lesions and tubular distension. Masson Trichrome (M&T) staining demonstrated 10 % more fibrosis and deposition of collagen in the cortex, the papilla, and the medulla in *Wnt4*$^{mCh/mCh}$ than the controls, and no fibrosis is observed in the newborn kidneys (Fig. 3A-B, Supplementary Figs. S9). Reduced transporter expression, like aquaporin, is typically associated with kidney fibrosis [2]. In line with this, aquaporin 1 (Aqp1) and proximal tubule (PT) markers *Lotus Tetragonolobus* Lectin (LTL) and thiazide-sensitive Na^+-Cl^- cotransporter (NCC) protein expression were reduced in the *Wnt4*$^{mCh/mCh}$ kidneys (Fig. 3C-E). In contrast, expression of *Adenosine triphosphatase b1* (*Atpb1*) was induced (Fig. 3 E). At the same time, the presence of EMT markers highlights fibroblast-derived matrix deposition toward fibrosis due to deregulated Wnt4 function (Fig. 3F, G).

Primary kidney cultures were carried out to understand the role of Wnt4 signal in injured *Wnt4*$^{mCh/mCh}$ kidneys. The primary TECs cultures derived from WT and *Wnt4*$^{mCh/mCh}$ kidneys [17] expressed *Wnt4, Aqp1*,

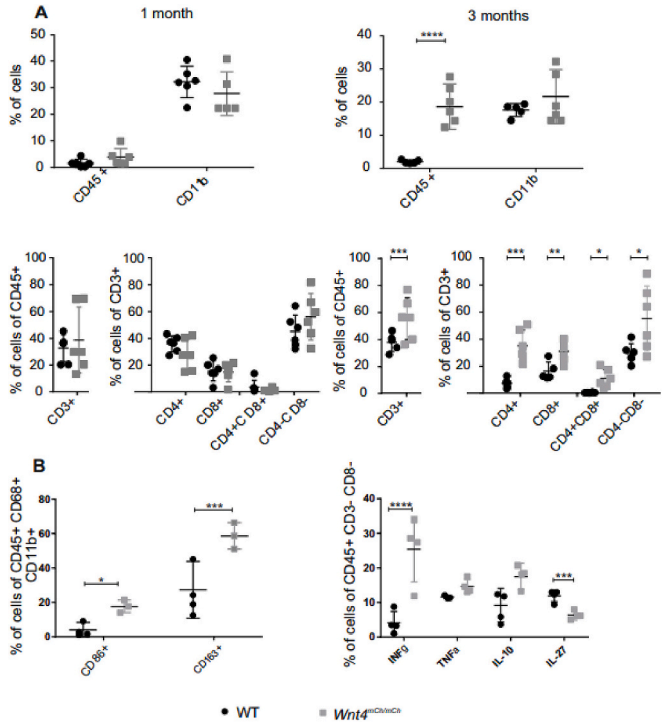

Fig. 5. EMT induces immune infiltration in *Wnt4*$^{mCh/mCh}$ fibrotic kidneys. A) Percentages of CD45+, CD11b+, CD3+, CD4+, CD8+, CD4+ CD8+ (Double positive cells), CD4- CD8- (Double negative cells, resident T-cells) in WT and *Wnt4*$^{mCh/mCh}$ kidneys. ($n = 6$ for WT; *Wnt4*$^{mCh/mCh}$ n = 6 at 1-month-old and $n = 5$ for WT; *Wnt4*$^{mCh/mCh}$ n = 6 at 3-month-old). B) CD86+, CD163+, INFg+, TNFa+, IL-10+ and IL27+ cells in WT and *Wnt4*$^{mCh/mCh}$ kidneys. ($n = 4$ for WT and *Wnt4*$^{mCh/mCh}$ $n = 3$ at 1-month-old and n = 4 for each genotype at 3-month-old). For the panel, data are presented as mean ± s.e.m. Two-way ANOVA with Tukey post-hoc analysis is used. *$P < 0.05$, **$P < 0.01$, ***$P < 0.001$, ****$P < 0.0001$.

E-cadherin and *α-SMA* mRNA and proteins (Supplementary Fig. S11). Interestingly the TECs of the *Wnt4*$^{mCh/mCh}$ kidneys induced in WT TECs showed alpha-smooth muscle (α-SMA), vimentin and fibronectin expression, epithelial cell markers (Fig. 4A). Moreover, the cytokeratin 8 (Troma1) was expressed in the epithelial kidney cells of adult *Wnt4*$^{mCh/mCh}$ mice in a Wnt4 dependent manner; confirming the roles of Wnt4 in MET/EMT control (Fig. 4B) while Tgf-β expression involved in fibrosis [27] remained unchanged irrespective of *Wnt4 mCherry* signaling (Fig. 3G, Supplementary Fig. S9). Consistent with the noted phenotypes, we identified increased α-SMA expression in the kidneys from *Wnt4*$^{mCh/mCh}$ mice as depicted by immunostaining, western blot and flow cytometric studies (Fig. 4C).

Since changes in the cell cycle are associated with the CKD in the TECs becoming arrested to the G2/M [2,4,28,29] we analyzed the cell cycle components and found increased Cyclin Dependent Kinase Inhibitor 1 (Cdkn1, p21) (Fig. 4D), expression of phospho-histone H3 (pH 3) in the cytokeratin 8 or Troma1 positive epithelial cells by flow cytometry indicating an extended G2/M phase (Fig. 4E). The energy consumption in TECs is connected to overall cellular activity. When reduced, it compromises their regenerative potential over fibrosis [30]. Changes in the mitochondria of the TECs derived from the *Wnt4*$^{mCh/mCh}$ mice depicted reduced ATP production (Supplementary Fig. S12). The noted deregulated Wnt4 signaling phenotypes are unlikely mediated by the canonical Wnt signaling pathway since the expression of a panel of canonical pathway Wnt genes and β-catenin protein showed opposite results than earlier reported to be associated with CKD development (Supplementary Fig. S13).

3.5. Kidney immune infiltration in the *Wnt4*$^{mCh/mCh}$ mice

Given the role of inflammation in fibrosis [31], we next used flow cytometry to study putative changes in kidney infiltration by the immune system cells. The proportion of CD45+ leukocytes was increased while CD11b+ macrophages remained normal in the kidneys of *Wnt4*$^{mCh/mCh}$ mice at three-month-old (Fig. 5A, Supplementary Fig. S14). However, the analysis showed more activated CD3 + CD4- CD8- double negative (DN) T lymphocytes (58 %), while the amount of the resident T cells in WT kidneys was 18–32 % [25,32]. The portion of the CD3+, the CD4 +, and the cytotoxic CD8+ T cells and those of the macrophages expressing CD11b+, CD68+ (M1), and CD11b and CD163 (M2) were also elevated. The DN cells expressed INFγ robustly while IL27 was reduced (Fig. 5B), especially at three months in the *Wnt4*$^{mCh/mCh}$ mice compared to controls. The infiltration of the immune cells to the W*nt4*$^{mCh/mCh}$ kidneys appeared more specific to the kidney, as no observed changes were seen in the spleen (Supplementary Fig. S15).

3.6. Fibrogenesis and partial EMT in *Wnt4*$^{mCh/mCh}$ kidneys suggest roles of Ca^{2+}/Calcineurin in signaling

To target the model of Wnt4 signal transduction in the TECs, the *Wnt4* and *Wnt4mCherry* vectors were transfected with the *SuperTopFlash Wnt* reporter to the Chinese hamster ovarian (CHO) cells. In line with the *in vivo* data, the *Wnt4mCherry* expressing cells highly downregulated the non-canonical Wnt pathway reporter expression compared to the control or cells transduced with wild-type *Wnt4* expression construct (Supplementary Fig. S16).

We first assayed the intracellular calcium (Ca^{2+}) stores [33]. Thapsigargin inhibits the sarcoplasmic/endoplasmic reticulum Ca -ATPase (SERCA), and the ionomycin Ca^{2+} ionophore depletes Ca^{2+} stores in cultured TECs. While the initial rate of calcium influx was similar in primary TECs, a more sustained and slower return to baseline Ca^{2+} levels in the *Wnt4*$^{mCh/mCh}$ primary TECs was observed with thapsigargin. To reach the Ca^{2+} peak in *Wnt4*$^{mCh/mCh}$ primary TECs, it took more time, and the velocity of releasing Ca^{2+} was slower in *Wnt4*$^{mCh/mCh}$ primary TECs than in WT cultured TECs (Fig. 6A). A similar result is observed for ionomycin, which depicted Ca^{2+} influx from intracellular stores. The amplitude of the initial peak representing store depletion from the ER appeared significantly higher in these *Wnt4*$^{mCh/mCh}$ primary TECs cells (Fig. 6B).

We then measured the expression of those genes implicated in the storage of Ca^{2+}, receptor-mediated entry in part controlled by the calcineurin (CaN) [34]. The studies showed that *mRNA* expressions of Ca^{2+} sensors *Stromal interaction molecule 1* (*Stim1*) and *Transient Receptor Potential Cation Channel Subfamily C Member 6* (*Trpc6*) were upregulated, whereas conversion of adenosine triphosphate to cyclic adenosine monophosphate (cAMP) *Adenylyl Cyclase 6* (*Ac6*), *Trpc1* were downregulated (Fig. 6C). Furthermore, Ca^{2+} and its intracellular receptor calmodulin (CaM) are required for cell cycle control, in the G1 and the G2 phase [34]. Given this, we evaluated CAM kinase and calcineurin (CaN) expression *in vivo*. We found that while CAM kinase remained unchanged, CaN expression was upregulated at the age of one month in mice but downregulated at the age of three months (Fig. 6D).

3.7. Calcineurin activated NFATc1- and TFEB-signaling pathways in the *Wnt4*$^{mCh/mCh}$ kidneys

Calcineurin controls the dephosphorylation of the *Nuclear factor of activated T-cells, cytoplasmic* (*1Nfatc-1c*), and *Transcription Factor EB* (*Tfeb*) connected to their nuclear localization [34,35]. *Nfatc-1c* and *Tfeb* transcription factors were upregulated in the kidneys of *Wnt4*$^{mCh/mCh}$ mice, and this was the case with the NFTAC-1 protein as well (Fig. 7A, B). The Tfeb regulates specific Wnt target genes, and its entry into the nucleus is coordinated by CaN mediated dephosphorylation [36]. The Tfeb-target genes are connected to Ca^{2+} signaling and cation channels

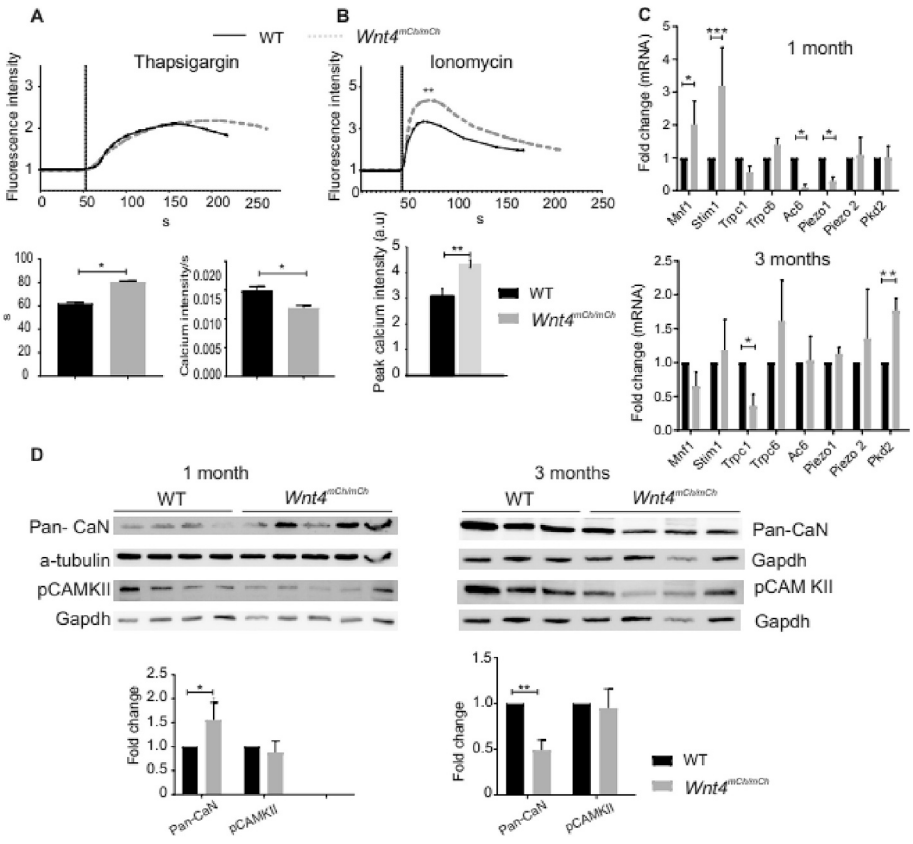

Fig. 6. Calcium controls the EMT program. A, B) Cytoplasmic calcium dynamics in TECs of WT and *Wnt4*$^{mCh/mCh}$ kidneys. Ca^{2+} measurement as in response to extracellular application of Thapsigargin (A) and ionomycin (B). Average time and velocity were assayed after Thapsigargin-induced Ca^{2+}, and the average amplitude of ionomycin-induced Ca^{2+} responses measured in WT and *Wnt4*$^{mCh/mCh}$ kidneys. Measurements were done in 4 independent experiments with the number of cells = 26 WT and 67 *Wnt4*$^{mCh/mCh}$. C) Fold change of the indicated genes in *Wnt4*$^{mCh/mCh}$ kidneys compared to WT kidneys. D) Protein expression of Pan-Calcineurin (CaN) and pCAM KII genes in 1- and 3-month-old kidneys. Western blot (up) and quantitation (down) of one-quarter of the kidney. (n = 4 for WT; *Wnt4*$^{mCh/mCh}$ n = 5 at 1-month-old and n = 3 for WT; *Wnt4*$^{mCh/mCh}$ n = 4 at 3-month-old). For the 3-month-old samples, the same gel blot was used for detecting the 3 proteins (pan-CaN, pCAMKII, Gapdh). For panel A-D, data are presented as mean ± s.e.m.; C) Two-way ANOVA with Tukey post-hoc analysis is used. *$P < 0.05$, **$P < 0.01$, ***$P < 0.001$. A, B, D) unpaired two-tailed t-test P** < 0.01.

independent of β-catenin activity [36]. Strikingly a panel of the Tfeb-target genes including *Neuron Navigator 3* (*Nav3*), *Ankyrin 2* (*Ank2*), *ADP-Ribosyl transferase 5* (*Art5*), *Integrin Subunit Alpha 10* (*Itga10*), and *Transient Receptor Potential Cation Channel Subfamily V Member 1* (*Trpa1*) were upregulated in *Wnt4*$^{mCh/mCh}$ mice at the time points studied (Fig. 7C).

To confirm that CaN might be triggered by Wnt4 signal like in the *in vivo* mouse, we generated a cell line over-expressing *Wnt4* gene in mk3 kidney cells. These cells represent early metanephric mesenchyme and do not express *Wnt4* gene [19]. This construct contained IRESGFP and the transfected cells were sorted. 80 % of the sorted cells were Wnt4-IRESGFP positive cells (Supplementary Fig. 17A). The cells were either treated with calcium which pushes forward the calcium signaling, or ethylene glycol-bis (β-aminoethyl ether)-N,N,N′,N′-tetraacetic acid (EGTA) that is an inhibitor of calcium signaling. Pan-CaN was assessed by western blot assay. The protein expression level was higher in the cell overexpressing *Wnt4* gene in the control and treated calcium cells, whereas EGTA treated cells had a reduced level similarly as in the control cells (Supplementary fig. 17B). The *in vitro* results confirmed that Wnt4 signal triggered the signaling pathway in the kidney cells based on calcium signaling.

To characterize the mechanisms of Wnt4 signal transduction in the TECs further, the TECs were cultured with cyclosporine-A (CSA) [37] and stained for the Nfatc-1 marker. Immunostaining depicted cytoplasmic localization of NFATC-1 in exposed *Wnt4*$^{mCh/mCh}$ cells, whereas expression was dominantly nucleolar in controls (Fig. 7D). CSA serves to inhibit Nfatc and Tfeb transcription factors. Therefore, we studied further the *Nav3*, *Ank2*, *Art5*, *Itag10*, and *Trpa1* target gene expression. In line with the depicted Nfat/Tfeb signal transduction cascade, CSA reduced the expression of these genes *in vitro* (Fig. 7E). The Tfeb-mediated Wnt target gene control depends on PARsylation (PARPs) activity [36]. We, therefore, subjected the *Wnt4*$^{mCh/mCh}$ and WT primary TECs with the Wnt signaling inhibitor of the PARPs activity, called XAV939 (XAV) a potent inhibitor of tankyrase enzymes, and included the lysosomal gene *Ppia* as a marker of Tfeb triggering lysosomal activity [36]. The treated TECs with XAV presented a decrease of *mRNA,* whereas after removal of Xav treatment and a further culture with fresh medium for 24 h, the levels of the previous expression were restored. As expected, the expression of *Ppia* was not affected by the treatment, and it is not dependent on the PARpsylation of Tfeb (Fig. 7F). We checked the protein level of phospho CaM and CaN content after the XAV treatment, and we observed that both proteins were reduced under the XAV treatment (Fig. 7G).

4. Discussion

In this study, we demonstrated that the expression of WNT4 after birth in adult kidneys contributes to kidney pathogenesis, renal fibrosis, and partial EMT development. Mechanistic investigations suggested that WNT4 re-expression promotes renal fibrogenesis *via* controlling EMT in TECs by enhancing likely the non-canonical Wnt signaling mechanism. Based on the Ca^{2+} signaling pathway analysis data, we hypothesize that

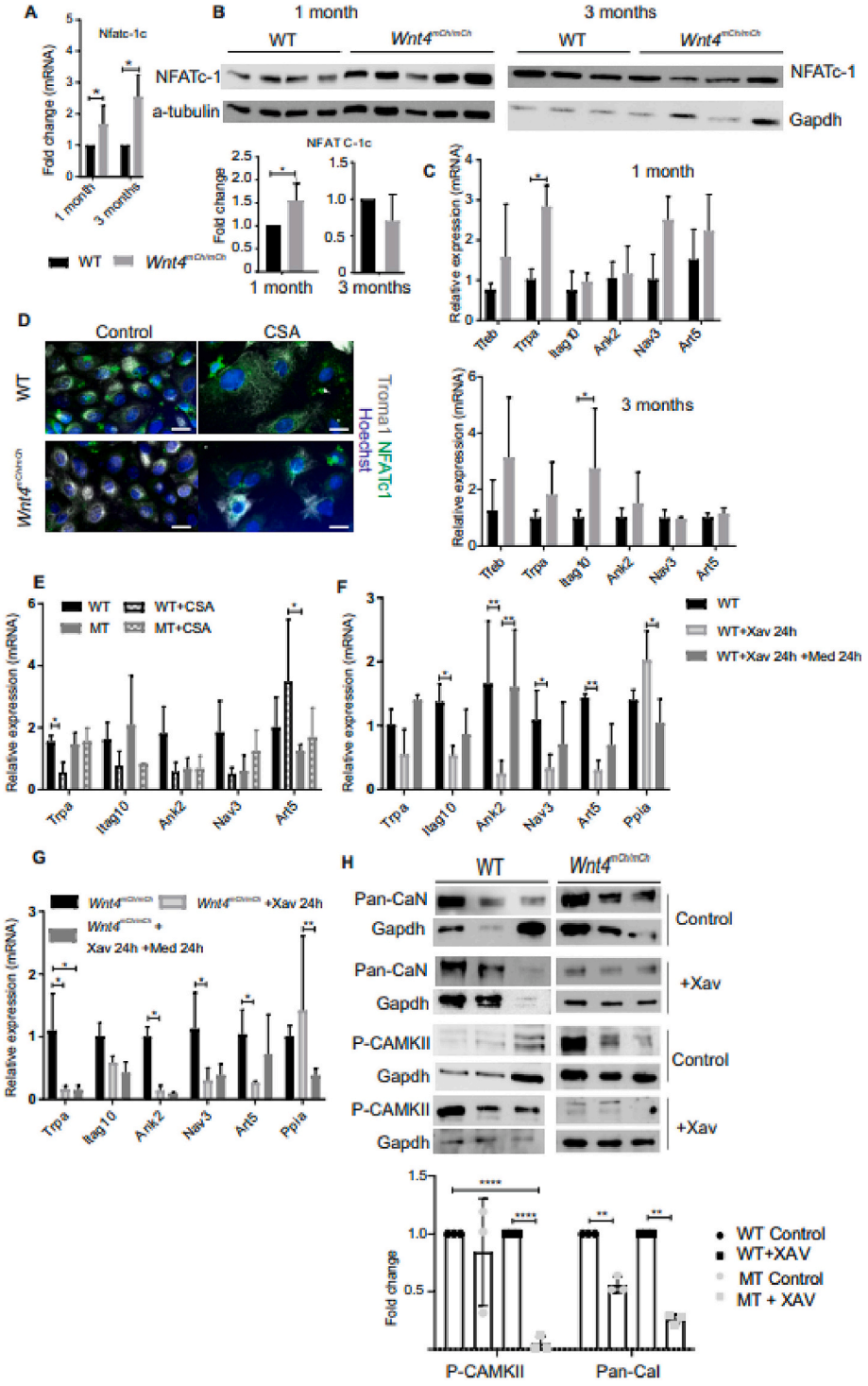

Fig. 7. Calcium triggers Nfat and Tfeb pathways. A) Fold change of *Nfatc-1c* gene in $Wnt4^{mCh/mCh}$ kidneys compared to WT kidneys ($n = 4$ for each genotype). B) NFTAC-1c protein expression in 1- and 3-month-old kidneys. Western blot and quantitation of one-quarter of the kidney. (n = 4 for WT; $Wnt4^{mCh/mCh}$ $n = 5$ at 1-month-old and $n = 3$ for WT; $Wnt4^{mCh/mCh}$ n = 4 at 3-month-old). C) Relative expression of the indicated Tfeb-mediated genes in $Wnt4^{mCh/mCh}$ kidneys compared to WT kidneys (n = 3 for each genotype). D) Representative images of immunolabeling for Troma1, Nfatc-1c and Hoechst in 1- and 3- month-old kidneys, (n = 3 for each genotype). Scale bar, 50 μm. E) Relative expression of the indicated Tfeb-mediated genes in treated TECs of $Wnt4^{mCh/mCh}$ kidneys compared to WT TECs with cyclosporine (CSA) (n = 3 for each genotype). F) Relative expression of the indicated Tfeb-mediated genes after 24 h culture of treated WT TECs with Wnt inhibitor (XAV) compared to control WT TECs (n = 3 for each genotype). G) Relative expression of the indicated Tfeb-mediated genes after 24 h culture of treated $Wnt4^{mCh/mCh}$ TECs with Wnt inhibitor (XAV) in compared to $Wnt4^{mCh/mCh}$ control TECs (n = 3 for each genotype). H) P-CAMKII and Pan-CaN protein expressions in TEC after 24 h culture of treated WT and $Wnt4^{mCh/mCh}$ TECs with Wnt inhibitor (XAV) compared to control WT and $Wnt4^{mCh/mCh}$ TECs (n = 3 for each genotype). For panel A-H, data are presented as mean ± s.e.m.; a, b) Unpaired two-tailed *t*-test P* < 0.05; C, e-h) Two-way ANOVA with Tukey post-hoc analysis was used. *$P < 0.05$, **$P < 0.01$, ****$P < 0.0001$.

the molecular mechanism of the WNT4 function is connected to the slow release of Ca^{2+} from the ER stores. This is linked to the dedifferentiation and proliferation of TECs leading to partial transition of the tubule epithelium toward mesenchymal characteristics. Furthermore, the deposition of proteins from the extracellular matrix (ECM) involved in the partial EMT was noted and the injured TECs intensify fibrogenesis establishment in the renal interstitium leading to the progression of CKD.

We found that Wnt4 signaling is connected to NFAT/Tfeb transcription factor expression changes *via* activating CaN protein. The results of *Wnt4*$^{mCh/mCh}$ transgenic mice suggest a novel and causal role of WNT4 in developing renal fibrosis through impacting Tfeb function and being independent of β-catenin. The newly discovered Wnt4 and Ca^{2+} links may also provide grounds for novel therapeutic approaches in renal fibrosis and CKD treatments. These possibilities are based on the findings that changes in Wnt4 signaling are connected to reactivated renal developmental control genes, the Ca^{2+} related ones, and those of the Wnt ones involved in the EMT process. WNT4 expression is also upregulated in the kidneys of CKD patients and, interestingly, is detectable in their urine. Hence, WNT4 may be an early-stage biomarker for CKD diagnostics [12,38].

Based on the current and published data, it now appears that WNT4 is initially inactive in the adult kidney but becomes induced upon renal injury [39]. Such ectopic WNT4 expression maintained in the cortex in the injured lesions may support kidney recovery. However, when Wnt4 signaling fails to be suppressed upon continued insults, such sustained Wnt function may promote partial dedifferentiation of the tubular epithelium to mesenchymal cells through the activated EMT process. This would lead to the expression of fibroblast cell-derived collagen matrix promoting fibrosis observed in the induced primary cultures of WT TEC by the *Wnt4*$^{mCh/mCh}$ TEC. The injured, matured tubules can degenerate toward a more immature state. In this process, the associated CaN activation may promote the reversion of these cells toward the gene pattern of a fetal kidney. In embryonic kidney development, calcium signaling is implicated in the development of the nephrons implying Nfat as a potential transcription factor regulating nephron formation [40,41]. In *Wnt4*$^{mCh/mCh}$ mice, such a process could potentially trigger together Nfat- and Tfeb-dependent transcriptional factors since these are known to be Wnt target genes [36]. We also observed an increase in cytosolic Ca^{2+} and *Stim1* mRNA in TECs. Given this, we hypothesize that Ca^{2+} *via* CaN will activate TFEB-mediated Wnt target genes. Indeed, overexpressed STIM/Orai1 channels can stimulate the Tfeb transcriptional program, constitutively active Orai1 channels, and fail to mediate Ca^{2+}-dependent inactivation increasing Ca^{2+} concentration in the cytosol [42].

To the best of our knowledge, this is the first study to demonstrate that Wnt4-inducing Ca^{2+} signaling pathways in adult TECs lead to partial EMT, renal fibrosis, and progression of CKD. More studies need to be carried out to increase our understanding of how the canonical and non-canonical Wnt pathways are involved in establishing and developing CKD, resulting in affine balance for rescuing injured TECs.

Funding

This work was supported by grants from for FN the Academy of Finland Profiling funding to the University of Oulu Profi3 (311934), Academy of Finland post-doctoral Fellowship (243014583), Foundations' Post Doc Pool (Svenska Kulturfonden), Finnish Cultural Foundation (Pekka ja Jukka-Pekka Lylykarin rahasto) and Magnus Ehrnrooth (24303464); and for SV by the Academy of Finland (206038, 121647, 250900, 613 260056, 24302880), Centre of Excellence Grant 2012–2017 of the Academy of Finland (251314), and Tekes BioRealHealth (24302443).

CRediT authorship contribution statement

Florence Naillat: Conceptualization, Formal analysis, Funding acquisition, Investigation, Methodology, Project administration, Resources, Supervision, Visualization, Writing – original draft, Writing – review & editing. **Ganga Deshar:** Formal analysis, Writing – original draft. **Anni Hankkila:** Formal analysis, Methodology. **Aleksandra Rak-Raszewska:** Formal analysis, Visualization, Writing – review & editing. **Abhishek Sharma:** Formal analysis. **Renata Prunskaite-Hyyrylainen:** Software. **Antti Railo:** Methodology. **Jingdong Shan:** Methodology. **Seppo J. Vainio:** Funding acquisition, Resources, Writing – review & editing.

Declaration of competing interest

None.

Data availability

No data was used for the research described in the article.

Acknowledgment

We would like to acknowledge the essential contributions of Johanna Kekolahti-Lias, Hannelle Hackman, Paula Harpenius, Sanna-Kaisa Kaajala for technical help, and Tina Jokela for taking part in the sampling of the *Wnt4*$^{mCh/mCh}$ kidneys. This work was carried out with the support of the Laboratory Animal Centre of the University of Oulu, the Biocenter Oulu Light Microscopy core facility, a member of Biocenter Finland's biological imaging platform services.

Appendix A. Supplementary data

Supplementary data to this article can be found online at https://doi.org/10.1016/j.bbadis.2024.167180.

References

[1] B. Bikbov, C.A. Purcell, A.S. Levey, M. Smith, A. Abdoli, M. Abebe, O.M. Adebayo, M. Afarideh, S.K. Agarwal, M. Agudelo-Botero, E. Ahmadian, Z. Al-Aly, V. Alipour, A. Almasi-Hashiani, R.M. Al-Raddadi, N. Alvis-Guzman, S. Amini, T. Andrei, C. L. Andrei, Z. Andualem, M. Anjomshoa, J. Arabloo, A.F. Ashagre, D. Asmelash, Z. Ataro, M.M.d.W. Atout, M.A. Ayanore, A. Badawi, A. Bakhtiari, S.H. Ballew, A. Balouchi, M. Banach, S. Barquera, S. Basu, M.T. Bayih, N. Bedi, A.K. Bello, I. M. Bensenor, A. Bijani, A. Boloor, A.M. Borzì, L.A. Cámera, J.J. Carrero, F. Carvalho, F. Castro, F. Catalá-López, A.R. Chang, K.L. Chin, S.C. Chung, M. Cirillo, E. Cousin, L. Dandona, R. Dandona, A. Daryani, R. das Gupta, F. M. Demeke, G.T. Demoz, D.M. Desta, H.P. Do, B.B. Duncan, A. Eftekhari, A. Esteghamati, S.S. Fatima, J.C. Fernandes, E. Fernandes, F. Fischer, M. Freitas, M. M. Gad, G.G. Gebremeskel, B.M. Gebresillassie, B. Geta, M. Ghafourifard, A. Ghajar, N. Ghith, P.S. Gill, I.A. Ginawi, R. Gupta, N. Hafezi-Nejad, A. Haj-Mirzaian, A. Haj-Mirzaian, N. Hariyani, M. Hasan, M. Hasankhani, A. Hasanzadeh, H.Y. Hassen, S.I. Hay, B. Heidari, C. Herteliu, C.L. Hoang, M. Hosseini, M. Hostiuc, S.S.N. Irvani, S.M.S. Islam, N. Jafari Balalami, S.L. James, S.K. Jassal, V. Jha, J. B. Jonas, F. Joukar, J.J. Jozwiak, A. Kabir, A. Kahsay, A. Kasaeian, T.D. Kassa, H. G. Kassaye, Y.S. Khader, R. Khalilov, E.A. Khan, M.S. Khan, Y.H. Khang, A. Kisa, C. P. Kovesdy, B. Kuate Defo, G.A. Kumar, A.O. Larsson, L.L. Lim, A.D. Lopez, P. A. Lotufo, A. Majeed, R. Malekzadeh, W. März, A. Masaka, H.A.A. Meheretu, T. Miazgowski, A. Mirica, E.M. Mirrakhimov, P. Mithra, B. Moazen, D. K. Mohammad, R. Mohammadpourhodki, S. Mohammed, A.H. Mokdad, L. Morales, I. Moreno Velasquez, S.M. Mousavi, S. Mukhopadhyay, J.B. Nachega, G. N. Nadkarni, J.R. Nansseu, G. Natarajan, J. Nazari, B. Neal, R.I. Negoi, C. T. Nguyen, R. Nikbakhsh, J.J. Noubiap, C. Nowak, A.T. Olagunju, A. Ortiz, M. O. Owolabi, R. Palladino, M. Pathak, H. Poustchi, S. Prakash, N. Prasad, A. Rafiei, S.B. Raju, K. Ramezanzadeh, S. Rawaf, D.L. Rawaf, L. Rawal, R.C. Reiner, A. Rezapour, D.C. Ribeiro, L. Roever, D. Rothenbacher, G.M. Rwegerera, S. Saadatagah, S. Safari, B.W. Sahle, H. Salem, J. Sanabria, I.S. Santos, A. Sarveazad, M. Sawhney, E. Schaeffner, M.I. Schmidt, A.E. Schutte, S. G. Sepanlou, M.A. Shaikh, Z. Sharafi, M. Sharif, A. Sharifi, D.A.S. Silva, J.A. Singh, N.P. Singh, M.M.M. Sisay, A. Soheili, I. Sutradhar, B.F. Teklehaimanot, B. etsay Tesfay, G.F. Teshome, J.S. Thakur, M. Tonelli, K.B. Tran, B.X. Tran, C. Tran Ngoc, I. Ullah, P.R. Valdez, S. Varughese, T. Vos, L.G. Vu, Y. Waheed, A. Werdecker, H.F. Wolde, A.B. Wondmieneh, S. Wulf Hanson, T. Yamada, Y. Yeshaw, N. Yonemoto, H. Yusefzadeh, Z. Zaidi, L. Zaki, S. bin Zaman,

N. Zamora, A. Zarghi, K.A. Zewdie, J. Ärnlöv, J. Coresh, N. Perico, G. Remuzzi, C.J. L. Murray, Global, regional, and national burden of chronic kidney disease, 1990–2017: a systematic analysis for the Global Burden of Disease Study 2017, Lancet 395 (2020), https://doi.org/10.1016/S0140-6736(20)30045-3.
[2] S. Lovisa, V.S. LeBleu, B. Tampe, H. Sugimoto, K. Vadnagara, J.L. Carstens, C. C. Wu, Y. Hagos, B.C. Burckhardt, T. Pentcheva-Hoang, H. Nischal, J.P. Allison, M. Zeisberg, R. Kalluri, Epithelial-to-mesenchymal transition induces cell cycle arrest and parenchymal damage in renal fibrosis, Nat. Med. 21 (2015), https://doi.org/10.1038/nm.3902.
[3] S.-S. Li, Q. Sun, M.-R. Hua, P. Suo, J.-R. Chen, X.-Y. Yu, Y.-Y. Zhao, Targeting the Wnt/β-catenin signaling pathway as a potential therapeutic strategy in renal tubulointerstitial fibrosis, Front. Pharmacol. 12 (2021), https://doi.org/10.3389/fphar.2021.719880.
[4] L. Hu, M. Ding, W. He, Emerging therapeutic strategies for attenuating tubular EMT and kidney fibrosis by targeting Wnt/β-catenin signaling, Front. Pharmacol. 12 (2022), https://doi.org/10.3389/fphar.2021.830340.
[5] J. He, S. Xu, M. Jiang, T. Wang, Y. Zhang, Z. Jia, M. Bai, A. Zhang, CDC20 inhibition alleviates fibrotic response of renal tubular epithelial cells and fibroblasts by regulating nuclear translocation of β-catenin, Biochim. Biophys. Acta (BBA) - Mol. Basis Dis. 2023 (1869) 166663, https://doi.org/10.1016/j.bbadis.2023.166663.
[6] S.J. Schunk, J. Floege, D. Fliser, T. Speer, WNT–β-catenin signalling — a versatile player in kidney injury and repair, Nat. Rev. Nephrol. 17 (2021) 172–184, https://doi.org/10.1038/s41581-020-00343-w.
[7] M.P. Rastaldi, Epithelial-mesenchymal transition and its implications for the development of renal tubulointerstitial fibrosis, J. Nephrol. 19 (2006).
[8] K. Stark, S. Vainio, G. Vassileva, A.P. McMahon, Epithelial transformation of metanephric mesenchyme in the developing kidney regulated by Wnt-4, Nature 372 (1994), https://doi.org/10.1038/372679a0.
[9] A. Kispert, S. Vainio, A.P. McMahon, Wnt-4 is a mesenchymal signal for epithelial transformation of metanephric mesenchyme in the developing kidney, Development 125 (1998), https://doi.org/10.1242/dev.125.21.4225.
[10] D.P. DiRocco, A. Kobayashi, M.M. Taketo, A.P. McMahon, B.D. Humphreys, Wnt4/β-catenin signaling in medullary kidney myofibroblasts, J. Am. Soc. Nephrol. 24 (2013), https://doi.org/10.1681/ASN.2012050512.
[11] K. Surendran, S.P. McCaul, T.C. Simon, A role for Wnt-4 in renal fibrosis, Am. J. Physiol. Renal Physiol. 282 (2002), https://doi.org/10.1152/ajprenal.0009.2001.
[12] J. Kiewisz, A. Skowronska, A. Winiarska, A. Pawlowska, J. Kiezun, A. Rozicka, A. Perkowska-Ptasinska, Z. Kmiec, T. Stompor, WNT4 expression in primary and secondary kidney diseases: dependence on staging, Kidney Blood Press. Res. 44 (2019), https://doi.org/10.1159/000498989.
[13] R. Prunskaite-Hyyryläinen, I. Skovorodkin, Q. Xu, I. Miinalainen, J. Shan, S. J. Vainio, Wnt4 coordinates directional cell migration and extension of the müllerian duct essential for ontogenesis of the female reproductive tract, Hum. Mol. Genet. 25 (2015), https://doi.org/10.1093/hmg/ddv621.
[14] W.F. Rodrigues, C.B. Miguel, M.H. Napimoga, C.J.F. Oliveira, J.E. Lazo-Chica, Establishing standards for studying renal function in mice through measurements of body size-adjusted creatinine and urea levels, Biomed. Res. Int. 2014 (2014) 1–8, https://doi.org/10.1155/2014/872827.
[15] S.M. Myllymäki, T.P. Teräväinen, A. Manninen, Two distinct integrin-mediated mechanisms contribute to apical lumen formation in epithelial cells, PloS One 6 (2011), https://doi.org/10.1371/journal.pone.0019453.
[16] T. Pikkarainen, T. Nurmi, T. Sasaki, U. Bergmann, S. Vainio, Role of the extracellular matrix-located Mac-2 binding protein as an interactor of the Wnt proteins, Biochem. Biophys. Res. Commun. 491 (2017), https://doi.org/10.1016/j.bbrc.2017.07.141.
[17] W. Ding, K. Yousefi, L.A. Shehadeh, Isolation, characterization, and high throughput extracellular flux analysis of mouse primary renal tubular epithelial cells, J. Vis. Exp. 2018 (2018), https://doi.org/10.3791/57718.
[18] F. Naillat, H. Saadeh, J. Nowacka-Woszuk, L. Gahurova, F. Santos, S. ichi Tomizawa, G. Kelsey, Oxygen concentration affects de novo DNA methylation and transcription in in vitro cultured oocytes, Clin Epigenetics 13 (2021), https://doi.org/10.1186/s13148-021-01116-3.
[19] M. Todd Valerius, Larry T. Patterson, David P. Witte, S. Steven Potter, Microarray analysis of novel cell lines representing two stages of metanephric mesenchyme differentiation, Mech. Dev. 112 (2002) 219–232.
[20] A. Railo, I.I. Nagy, P. Kilpeläinen, S. Vainio, Wnt-11 signaling leads to down-regulation of the Wnt/β-catenin, JNK/AP-1 and NF-κB pathways and promotes viability in the CHO-K1 cells, Exp. Cell Res. 314 (2008) 2389–2399, https://doi.org/10.1016/J.YEXCR.2008.04.010.
[21] F. Naillat, W. Yan, R. Karjalainen, A. Liakhovitskaia, A. Samoylenko, Q. Xu, Z. Sun, B. Shen, A. Medvinsky, S. Quaggin, S.J. Vainio, Identification of the genes regulated by Wnt-4, a critical signal for commitment of the ovary, Exp. Cell Res. 332 (2015), https://doi.org/10.1016/j.yexcr.2015.01.010.
[22] V. Veikkolainen, N. Ali, M. Doroszko, A. Kiviniemi, I. Miinalainen, C. Ohlsson, M. Poutanen, N. Rahman, K. Elenius, S.J. Vainio, F. Naillat, Erbb4 regulates the oocyte microenvironment during folliculogenesis, Hum. Mol. Genet. 29 (2020), https://doi.org/10.1093/hmg/ddaa161.
[23] R. Prunskaite-Hyyryläinen, Optical projection tomography imaging to study kidney organogenesis, in, Methods Mol. Biol. (2019), https://doi.org/10.1007/978-1-4939-9021-4_16.
[24] I.I. Nagy, Q. Xu, F. Naillat, N. Ali, I. Miinalainen, A. Samoylenko, S.J. Vainio, Impairment of Wnt11 function leads to kidney tubular abnormalities and secondary glomerular cystogenesis, BMC Dev. Biol. 16 (2016), https://doi.org/10.1186/s12861-016-0131-z.
[25] M.N. Martina, S. Noel, A. Saxena, S. Bandapalle, R. Majithia, C. Jie, L.J. Arend, M. E. Allaf, H. Rabb, A.R.A. Hamad, Double-negative αβ T cells are early responders to AKI and are found in human kidney, J. Am. Soc. Nephrol. 27 (2016), https://doi.org/10.1681/ASN.2014121214.
[26] A. Roy, A. Kucukural, Y. Zhang, I-TASSER: a unified platform for automated protein structure and function prediction, Nat. Protoc. 5 (2010), https://doi.org/10.1038/nprot.2010.5.
[27] A. Akhmetshina, K. Palumbo, C. Dees, C. Bergmann, P. Venalis, P. Zerr, A. Horn, T. Kireva, C. Beyer, J. Zwerina, H. Schneider, A. Sadowski, M.O. Riener, O. A. MacDougald, O. Distler, G. Schett, J.H.W. Distler, Activation of canonical Wnt signalling is required for TGF-β-mediated fibrosis, Nat. Commun. 3 (2012), https://doi.org/10.1038/ncomms1734.
[28] L. Yang, T.Y. Besschetnova, C.R. Brooks, J.v. Shah, J.v. Bonventre, Epithelial cell cycle arrest in G2/M mediates kidney fibrosis after injury, Nat. Med. 16 (2010), https://doi.org/10.1038/nm.2144.
[29] G. Canaud, J.v. Bonventre, Cell cycle arrest and the evolution of chronic kidney disease from acute kidney injury, Nephrol. Dial. Transplant. 30 (2015), https://doi.org/10.1093/ndt/gfu230.
[30] H. Mi Kang, S. Ho Ahn, P. Choi, Y.-A. Ko, S. Hyeok Han, F. Chinga, A. Seo Deok Park, J. Tao, K. Sharma, J. Pullman, E.P. Bottinger, I.J. Goldberg, K. Susztak, Defective Fatty Acid Oxidation in Renal Tubular Epithelial Cells has a Key Role in Kidney Fibrosis Development, 2014, https://doi.org/10.1038/nm.3762.
[31] T.A. Wynn, Invited review cellular and molecular mechanisms of fibrosis, Journal of Pathology, J. Pathol. 214 (2008) 199–210, https://doi.org/10.1002/path.2277.
[32] D.B. Ascon, M. Ascon, S. Satpute, S. Lopez-Briones, L. Racusen, R.B. Colvin, M. J. Soloski, H. Rabb, Normal mouse kidneys contain activated and CD3 + CD4 − CD8 − double-negative T lymphocytes with a distinct TCR repertoire, J. Leukoc. Biol. 84 (2008), https://doi.org/10.1189/jlb.0907651.
[33] A. Takahashi, P. Camacho, J.D. Lechleiter, B. Herman, Measurement of intracellular calcium, Physiol. Rev. 79 (1999), https://doi.org/10.1152/physrev.1999.79.4.1089.
[34] C.R. Kahl, A.R. Means, Regulation of cell cycle progression by calcium/calmodulin-dependent pathways, Endocr. Rev. 24 (2003), https://doi.org/10.1210/er.2003-0008.
[35] R. Schober, L. Waldherr, T. Schmidt, A. Graziani, C. Stilianu, L. Legat, K. Groschner, R. Schindl, STIM1 and Orai1 regulate Ca 2+ microdomains for activation of transcription, Biochim. Biophys. Acta Mol. Cell Res. 1866 (2019), https://doi.org/10.1016/j.bbamcr.2018.11.001.
[36] S. Kim, G. Song, T. Lee, M. Kim, J. Kim, H. Kwon, J. Kim, W. Jeong, U. Lee, C. Na, S. Kang, W. Kim, J.K. Seong, E. hoon Jho, PARsylated transcription factor EB (TFEB) regulates the expression of a subset of Wnt target genes by forming a complex with β-catenin-TCF/LEF1, Cell Death Differ. 28 (2021), https://doi.org/10.1038/s41418-021-00770-7.
[37] X. Shen, Y. Zhang, C. Lin, C. Weng, Y. Wang, S. Feng, C. Wang, X. Shao, W. Lin, B. Li, H. Wang, J. Chen, H. Jiang, Calcineurin inhibitors ameliorate PAN-induced podocyte injury through the NFAT–Angptl4 pathway, J. Pathol. 252 (2020), https://doi.org/10.1002/path.5512.
[38] Y. Wang, S.L. Zhao, S.Y. Wei, Y.X. Wang, T.T. Diao, J.S. Li, Y.X. He, J. Yu, X. Y. Jiang, Y. Cao, X.Y. Mao, Q.J. Wei, B. Li, Wnt4 is a novel biomarker for the early detection of kidney tubular injury after ischemia/reperfusion injury, Sci. Rep. 6 (2016), https://doi.org/10.1038/srep32610.
[39] J. Kiewisz, A. Skowronska, A. Winiarska, A. Pawlowska, J. Kiezun, A. Rozicka, A. Perkowska-Ptasinska, Z. Kmiec, T. Stompor, WNT4 expression in primary and secondary kidney diseases: dependence on staging, Kidney Blood Press. Res. 44 (2019) 200–210, https://doi.org/10.1159/000498989.
[40] S.F. Burn, A. Webb, R.L. Berry, J.A. Davies, A. Ferrer-Vaquer, A.K. Hadjantonakis, N.D. Hastie, P. Hohenstein, Calcium/NFAT signalling promotes early nephrogenesis, Dev. Biol. 352 (2011), https://doi.org/10.1016/j.ydbio.2011.01.033.
[41] S. Tanigawa, H. Wang, Y. Yang, N. Sharma, N. Tarasova, R. Ajima, T.P. Yamaguchi, L.G. Rodriguez, A.O. Perantoni, Wnt4 induces nephronic tubules in metanephric mesenchyme by a non-canonical mechanism, Dev. Biol. 352 (2011), https://doi.org/10.1016/j.ydbio.2011.01.012.
[42] I. Frischauf, M. Litviňuková, R. Schober, V. Zayats, B. Svobodová, D. Bonhenry, V. Lunz, S. Cappello, L. Tociu, D. Reha, A. Stallinger, A. Hochreiter, T. Pammer, C. Butorac, M. Muik, K. Groschner, I. Bogeski, R.H. Ettrich, C. Romanin, R. Schindl, Transmembrane helix connectivity in Orai1 controls two gates for calcium-dependent transcription, Sci. Signal. 10 (2017), https://doi.org/10.1126/scisignal.aao0358.